

Distinct charge orders in the planes and chains of ortho-III ordered $\text{YBa}_2\text{Cu}_3\text{O}_{6+\delta}$ identified by resonant elastic x-ray scattering

A. J. Achkar,¹ R. Sutarto,^{2,3} X. Mao,¹ F. He,³ A. Frano,^{4,5} S. Blanco-Canosa,⁴ M. Le Tacon,⁴ G. Ghiringhelli,⁶ L. Braicovich,⁶ M. Minola,⁶ M. Moretti Sala,⁷ C. Mazzoli,⁶ Ruixing Liang,² D. A. Bonn,² W. N. Hardy,² B. Keimer,⁴ G. A. Sawatzky,² and D. G. Hawthorn^{1,*}

¹*Department of Physics and Astronomy, University of Waterloo, Waterloo, N2L 3G1, Canada*

²*Department of Physics and Astronomy, University of British Columbia, Vancouver, V6T 1Z4, Canada*

³*Canadian Light Source, University of Saskatchewan, Saskatoon, Saskatchewan, S7N 0X4, Canada*

⁴*Max-Planck-Institut für Festkörperforschung, Heisenbergstraße 1, D-70569 Stuttgart, Germany*

⁵*Helmholtz-Zentrum Berlin für Materialien und Energie,
Albert-Einstein-Straße 15, D-12489 Berlin, Germany*

⁶*CNR-SPIN, CNISM and Dipartimento di Fisica, Politecnico di Milano,
Piazza Leonardo da Vinci 32, I-20133 Milano, Italy*

⁷*European Synchrotron Radiation Facility, BP 220, F-38043 Grenoble Cedex, France*

Recently, quasi-static charge density wave (CDW) order in the CuO_2 planes of underdoped $\text{YBa}_2\text{Cu}_3\text{O}_{6+\delta}$ was detected using resonant soft x-ray scattering. An important question remains: is the chain layer responsible for this charge ordering? Here, we explore the energy and polarization dependence of the resonant scattering intensity in a detwinned sample of $\text{YBa}_2\text{Cu}_3\text{O}_{6.75}$ with ortho-III oxygen ordering in the chain layer. We show that the ortho-III CDW order in the chains is distinct from the CDW order in the planes. The ortho-III structure gives rise to a commensurate superlattice reflection at $Q=[0.33\ 0\ L]$ whose energy and polarization dependence agrees with expectations for oxygen ordering and a spatial modulation of the Cu valence in the chains. Incommensurate peaks at $[0.30\ 0\ L]$ and $[0\ 0.30\ L]$ from the CDW order in the planes are shown to be distinct in Q as well as their temperature, energy and polarization dependence, and are thus unrelated to the structure of the chain layer. Moreover, the energy dependence of the CDW order in the planes is shown to result from a spatial modulation of energies of the Cu $2p$ to $3d_{x^2-y^2}$ transition, similar to stripe-ordered 214 cuprates.

PACS numbers: 74.72.Gh, 61.05.cp, 71.45.Lr, 78.70.Dm

Direct evidence for charge density wave (CDW) order in $\text{YBa}_2\text{Cu}_3\text{O}_{6+\delta}$ (YBCO) was recently observed in high magnetic field using nuclear magnetic resonance [1] and in zero-field diffraction, first with resonant soft x-ray scattering (RSXS) [2] and subsequently with hard x-ray scattering [3]. Prior to these measurements, static density wave order [4, 5] had been observed in 214 cuprates ($\text{La}_{2-x-y}(\text{Ba},\text{Sr})_x(\text{Eu},\text{Nd})_y\text{CuO}_4$) [6] as well as $\text{Ca}_{2-x}\text{Na}_x\text{CuO}_2\text{Cl}_2$ [7] and $\text{Bi}_2\text{Sr}_2\text{CaCu}_2\text{O}_{8+\delta}$ [8]. However, density wave order in YBCO – a material long considered a benchmark cuprate due to its low disorder and high $T_{c,\text{max}} \simeq 94.2\text{ K}$ – had only been inferred indirectly, being offered as an explanation for Hall effect measurements [9] and the electron pockets observed in quantum oscillation experiments [10–12]. The observation of density wave order in YBCO thus marks an important milestone in efforts to determine whether density wave order is generic to the cuprates while providing new opportunities to identify common features of CDW order in the cuprates.

RSXS is well suited to give direct insight into the nature of CDW order in YBCO. RSXS involves diffrac-

tion with the photon energy tuned through an x-ray absorption edge. This gives significant energy dependence to the atomic scattering form factor, $f(\omega)$, enhancing the scattering from weak ordering and providing sensitivity to the charge, spin and orbital occupation of specific elements. At the Cu L absorption edge, the scattering is sensitive to modulations in the unoccupied Cu $3d$ states that are central to the low energy physics of the cuprates [13–17]. The recent RSXS measurements of Ghiringhelli *et al.* at the Cu L absorption edge identified quasi-static superlattice peaks at $Q = [0.31\ 0\ L]$ and $[0\ 0.31\ L]$ indicative of CDW order [2]. They also showed that the intensity of the superlattice reflections peak at $\sim T_c$ and decrease in intensity for $T < T_c$, providing a clear link between the density wave order and superconductivity [2]. Importantly, based on the energy dependence of the scattering intensity and the presence of peaks at $H=0.31$ and $K=0.31$ in a detwinned sample, Ghiringhelli *et al.* also demonstrate that the CDW superlattice peaks originate from modulations in the CuO_2 planes.

However, the possible role of the charge reservoir layer in stabilizing the CDW order is not yet clear. In YBCO, the charge reservoir for the CuO_2 planes is composed of CuO chains. The Cu sites in the chains (Cu1) and planes (Cu2) have different orbital symmetries and

* dhawthor@uwaterloo.ca.

contribute differently to x-ray absorption spectroscopy (XAS) and RSXS measurements [18, 19]. In addition to making the structure orthorhombic ($a \neq b$), the chain layer can be oxygen ordered into a variety of “ortho” ordered phases [20, 21]. For instance, the ortho-III phase corresponds to a repeated pattern of full–full–empty ordering of oxygen in the chains [see Fig. 1(a)] that produces a commensurate superlattice peak at $[0.33\ 0\ L]$, in close proximity to the $[0.31\ 0\ L]$ peaks observed in Ref. [2]. In addition, the chains may also be susceptible to CDW order along the chains (producing incommensurate peaks at $[0\ K\ L]$) [22–24]. As such, the chains may act to stabilize static CDW order in YBCO akin to the low-temperature tetragonal (LTT) structural phase stabilizing spin and charge stripes in stripe ordered 214 cuprates [6, 25].

In this letter, we present RSXS measurements of a high purity, ortho-III ordered single crystal of $\text{YBa}_2\text{Cu}_3\text{O}_{6.75}$ ($T_c=75.2\text{ K}$, $p=0.133$) [26, 27] that a) confirm the in-plane origin of the incommensurate $[0.30\ 0\ L]$ CDW peak [28], b) clarify its relation to the oxygen ordering in the chain layer and c) demonstrate a link to the microscopic origin of stripes in 214 cuprates. Analysis of the scattering intensities provides clear evidence that the $[0.30\ 0\ L]$ CDW peak has an energy, polarization and temperature dependence that is distinct from the $[0.33\ 0\ L]$ oxygen ordering peak, indicating there is no clear relation between the chain layer and the $[0.30\ 0\ L]$ CDW order. Moreover, the $[0.30\ 0\ L]$ peak is shown to result from a spatial modulation of the energy of the Cu $2p$ to $3d_{x^2-y^2}$ transition, unlike the $[0.33\ 0\ L]$ oxygen ordering peak, which is described by a spatial modulation of the Cu valence. The former is consistent with RSXS measurements in stripe ordered 214 cuprates [17], which is also described by the energy shift model, suggesting a common origin to the CDW order that is generic to the cuprates.

Resonant scattering measurements were performed at the Canadian Light Source’s REIXS beamline [29] using linearly polarized light in both σ and π scattering geometries, as depicted in Fig. 1(b). The sample orientation was confirmed by detection of $[0\ 0\ 1]$, $[\pm 1\ 0\ 2]$ and $[0\ \pm 1\ 2]$ Bragg reflections at 2.05 keV. XAS was measured using total fluorescence yield (TFY).

The measured intensity of H and K scans through the $[0.30\ 0\ 1.4]$ and $[0\ 0.30\ 1.4]$ peaks at 60 K is shown in Fig. 1(c) for the incident photon energies indicated in Fig. 1(d). These superlattice reflections are observed above a large x-ray fluorescence background, similar to measurements from Ref. 2. In addition, there is also a peak at $[0.33\ 0\ L]$ that is evident at higher photon energy.

The scattering intensity, I_{sc} , was determined by fitting the fluorescence background to a polynomial and subtracting it from the data [Fig. 1(e)]. This procedure was repeated as a function of photon energy and for both

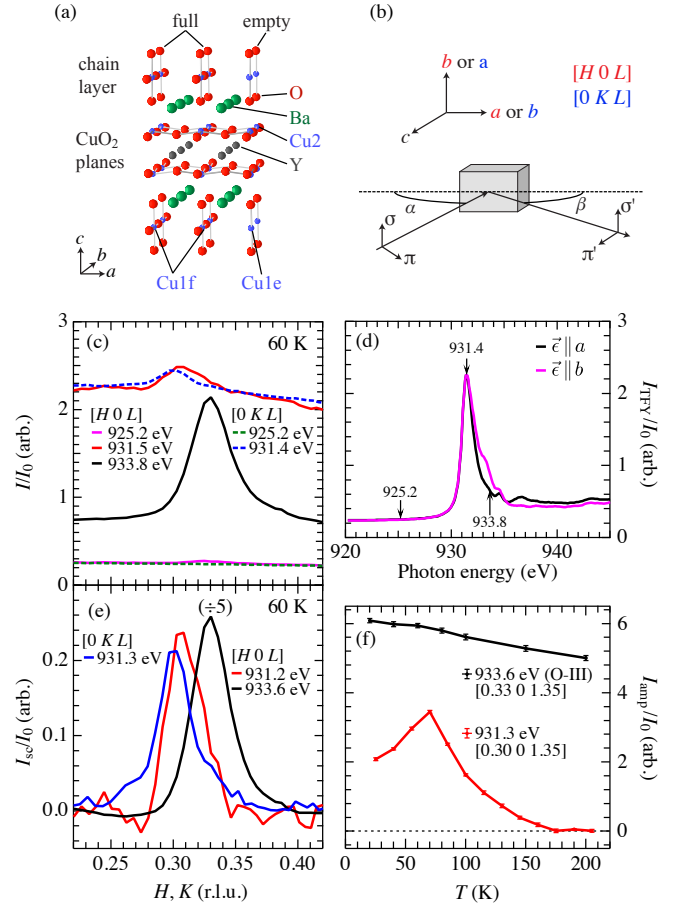


FIG. 1. (a) The crystal structure of ortho-III ordered YBCO. (b) A schematic of the experiment geometry. (c) $[H\ 0\ L]$ and $[0\ K\ L]$ scans at $T = 60\text{ K}$ measured using sigma polarized light through the $[0.30\ 0\ 1.4]$ and $[0\ 0.30\ 1.4]$ superlattice peaks, which appear when the photon energy is tuned to the peak of the XAS ($\sim 931.4\text{ eV}$). The ortho-III oxygen ordering superlattice peak is seen at $[0.33\ 0\ L]$ and is most prominent around 933.8 eV . (d) The x-ray absorption with polarization along the a and b axes measured using total fluorescence yield. (e) The scattering intensity with fluorescence background subtracted. (f) The temperature dependence of the amplitudes of the $[0.30\ 0\ 1.35]$ and $[0.33\ 0\ 1.35]$ peaks.

σ and π incident photon polarizations, as shown in Fig. 2. In Fig. 2(a) and 2(b), two peaks at $H=0.30$ and $H=0.33$ are observed that resonate at different energies and have a different polarization dependence. Due to the large width of both peaks, they overlap in H forming one broad asymmetric peak, which is particularly evident around the peak in the x-ray absorption (931.4 eV). In contrast, the peak at $[0\ 0.30\ 1.4]$, shown in Fig. 2(c) and 2(d), resonates at 931.3 eV with only a small signature of the peak at ~ 0.33 , likely due to residual ($<3\%$) twinning of the sample. From these scans at 60 K, the correlation lengths of the peaks are $\xi(K=0.30) \simeq 42\text{ \AA}$, $\xi(H=0.30) \simeq 40\text{ \AA}$ and $\xi(H=0.33) \simeq 37\text{ \AA}$. Consistent with previous

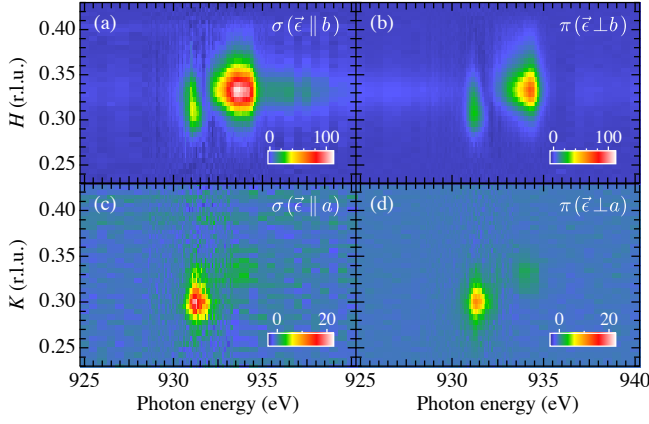


FIG. 2. The $[H\ 0\ L]$ [(a) and (b)] and $[0\ K\ L]$ [(c) and (d)] scattering intensity (measured intensity - fluorescence background) at $T = 60$ K measured with σ [(a) and (c)] and π [(b) and (d)] polarized light.

work [2], the amplitude of the $[0.30\ 0\ L]$ reflection is first distinguished from the fluorescence background at ~ 160 K, peaks at $\sim T_c$ and decreases for $T < T_c$, as shown in Fig. 1(f). In contrast, the $[0.33\ 0\ L]$ peak amplitude exhibits a gradual T dependence with no notable features at T_c or 160 K.

Analysis of the energy and polarization dependence of the integrated scattering intensities (Fig. 3) demonstrates that the $H=0.30$ and $K=0.30$ peaks are due to modulations in the CuO_2 planes, whereas the $H=0.33$ peaks are due to ortho-III ordering in the chain layer. To model the scattering intensity of the $H=0.33$ peak, we followed the procedure in Ref. 19 which illustrated that the scattering intensity and polarization dependence of the oxygen order superstructure in ortho-II ordered YBCO (full-empty-full-empty chains) could be calculated by accounting for the impact of the oxygen dopants on the $\text{Cu}1\ d$ states in the full and empty chains. This was done by experimentally determining the energy dependence of the atomic scattering tensor, F_i , for Cu in full, $F_{\text{Cu1f}}(\omega)$, and empty, $F_{\text{Cu1e}}(\omega)$, chains using polarization dependent x-ray absorption measurements in YBCO prepared with either an entirely full ($\text{YBa}_2\text{Cu}_3\text{O}_7$) or an entirely empty ($\text{YBa}_2\text{Cu}_3\text{O}_6$) chain layer. Here we use the same analysis for the $H = 0.33$ peak with $F_{\text{Cu1f}}(\omega)$ and $F_{\text{Cu1e}}(\omega)$ from Ref. 19 and $I_{\text{sc,o-III}}(H=0.33, \vec{\epsilon}) = |f_{\text{Cu1f}}(\omega, \vec{\epsilon}) + f_O - f_{\text{Cu1e}}(\omega, \vec{\epsilon})|^2$. As shown in Fig. 3(a), this analysis reproduces the energy and polarization dependence of the $H = 0.33$ peak, providing confirmation that this peak is dominated by the oxygen order in the chain layer.

In contrast, both the polarization and energy dependence of the $H=0.30$ and $K=0.30$ peaks are consistent with a spatial modulation of the $\text{Cu}\ 3d_{x^2-y^2}$ states in the CuO_2 planes. First, one must note that the incident π

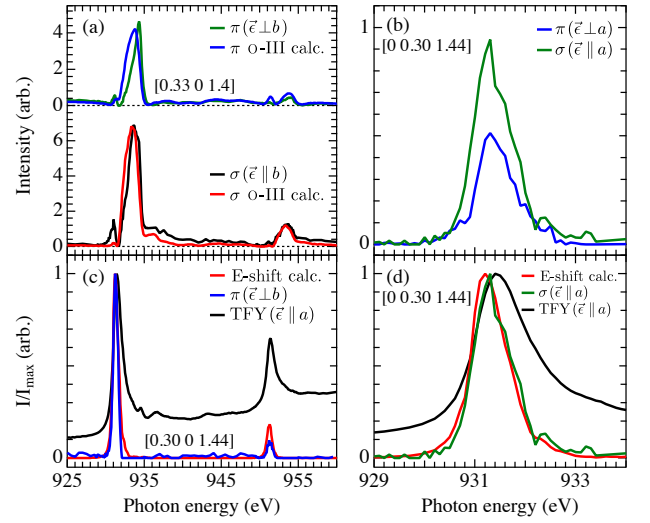


FIG. 3. (a) The measured energy dependence of the $[0.33\ 0\ 1.4]$ oxygen ordering peak with σ (black) and π (green) polarized incident light along with the calculated spectra for ortho-III oxygen ordering of the chain layer (red, blue). The π polarized data is offset for clarity. (b) The energy dependence of the $[0\ 0.30\ 1.44]$ peak measured with σ (green) and π (blue) polarized light. (c) The energy dependence of the $[0.30\ 0\ 1.44]$ peak (blue) with π polarized light compared to the energy shift model calculation (red). The energy shift calculation captures the correct peak position and energy width of the scattering intensity. (d) The energy shift model calculation (red) compared to the $[0\ 0.30\ 1.44]$ peak (green) with σ polarized light.

and σ polarizations couple to different components of the scattering tensor. For σ polarization, the photon polarization is entirely along the $b(a)$ axis for the $H(K) = 0.30$ peak and is therefore sensitive to the $bb(aa)$ components of the scattering tensor. However for π polarized light, the polarization has components along both the a and c axes that depend on the scattering geometry. For modulations of $\text{Cu}\ 3d_{x^2-y^2}$ states, $f_{aa,\text{Cu}2} \simeq f_{bb,\text{Cu}2} \gg f_{cc,\text{Cu}2}$ and $I_{\text{sc}}(\pi\pi')/I_{\text{sc}}(\sigma\sigma') = [\sin(\alpha)\sin(\beta)\Delta f_{aa}]^2$, where α and β are the angles of the incident and scattered light relative to the sample surface [see Fig. 1(b)]. [30] For the values of α and β in our measurement, one would expect the ratio of $f(\pi\pi')/f(\sigma\sigma') = 0.46$ for a modulation of $\text{Cu}\ 3d_{x^2-y^2}$ states. As shown in Fig. 3(b), the $K = 0.30$ peak is in good agreement with this ratio.

A final intriguing aspect of the energy dependence of the scattering intensity is that the lineshape can be described by a simple phenomenological model for the scattering intensity based on a spatial modulation of the energy of the $\text{Cu}\ 2p$ to $3d_{x^2-y^2}$ transition. The energy of this transition is determined by the energy of the $3d_{x^2-y^2}$ states, as well as the core hole energy and the interaction energy of the core hole with the d electrons, all of which may be spatially modulated. This energy shift model was

recently shown to account for the energy dependence of the scattering intensity of the $[1/4\ 0\ L]$ charge stripe ordering peak in $\text{La}_{1.475}\text{Nd}_{0.4}\text{Sr}_{0.125}\text{CuO}_4$, unlike models based on lattice displacements or charge density modulations [17]. Although in YBCO we do not know the structure factor that accounts for the $[0.30\ 0\ L]$ and $[0\ 0.30\ L]$ peaks, we can naively invoke the same energy shift model and assume that $I_{\text{sc}}[0.30\ 0\ L](\omega) \propto I_{\text{sc}}[0\ 0.30\ L](\omega) \propto |f_{\text{Cu2a}}(\hbar\omega + \Delta E) - f_{\text{Cu2b}}(\hbar\omega - \Delta E)|^2$, where Cu2a and Cu2b represent two sites in the CuO_2 planes with $f(\omega)$ that is identical apart from a small energy shift $\pm\Delta E$ at each site. Following previous work, $f_{\text{Cu2}}(\omega)$ can be determined from the experimentally measured x-ray absorption spectra [13, 14, 17]. In this case, the XAS with polarization oriented along the a -axis of the sample is used since it is dominated by the $\text{Cu } 3d_{x^2-y^2}$ states of the CuO_2 planes with minimal chain contribution. As shown in Fig. 3(c) and 3(d), the energy shift model is in excellent agreement with the experiment, capturing the correct energy dependence and peak position, which peaks ~ 0.1 eV below the L_3 peak of the x-ray absorption. Note, for this calculation $\Delta E = 0.1$ eV was used (See [31]).

Although the energy shifts, and thus the scattering, may ultimately be caused by a modulation in Cu valence, the microscopic origin of the energy shifts is currently unclear. An important implication of the energy shift model is that the resonant scattering provides only indirect evidence for charge density (valence) modulations – the success of the energy shift model allows one to infer there is a charge density modulation since this must occur if the electronic structure is spatially modulated [17]. In contrast, the energy dependence of the ortho-III oxygen order peak ($H = 0.33$) is described “directly” in terms of a large change in valence between Cu in the full and empty chains. However, since we cannot presently estimate the magnitude of the charge density modulation from the energy shifts, it is conceivable that a modulation of charge is not the central feature of the newfound density wave order in YBCO (and also stripes in 214 cuprates). In such a case, the energy shifts may in fact be a signature of a novel electronic state, such as a valence bond solid [17]. Alternately, the energy shifts may result from weak-coupling, Fermi surface reconstruction descriptions of density wave order in the cuprates. Regardless of the origin, the success of the energy shift model may imply that the temperature dependence of the peak amplitudes results from a temperature dependent energy shift that peaks at T_c , providing an apparent link between the energy shifts and superconductivity.

Moreover, the applicability of the energy shift model to the resonant scattering intensity of charge stripe order in 214 cuprates and YBCO indicates that the CDW order likely shares a common origin in the two material systems. This commonality stands in contrast to important differences between the density wave order in YBCO

and stripe ordered 214 cuprates. In 214 cuprates, the charge order is stabilized by the LTT structural phase [6, 32], has an incommensurability that plateaus at high doping at the commensurate value of $2\delta = 0.25$ [5, 33] and is understood to be unidirectional in nature (i.e. stripes). In YBCO, while there is no LTT phase, one might expect that the orthorhombic structure of YBCO would preferentially stabilize stripe order propagating along the a or b axes, perhaps with a period locked to the oxygen ordering in the chain layer of YBCO. However, no clear link between structure and the H and $K = 0.30$ peaks is observed in our measurements. Rather, the incommensurate value of the $2\delta = 0.30$ peaks relative to the commensurate oxygen ordering peak at $H = 0.33$, the similar magnitude of the scattering intensity of the H and K peaks and the presence of the $H = 0.30$ peaks in samples with weak oxygen order (only very short range ortho-V order) [2], indicate that the structural distortions are not an essential ingredient for CDW order in YBCO. Additionally, the existence of peaks along both H and K would seem to favour 2D checkerboard order. However, if the connection to the lattice is indeed weak, domains of unidirectional stripes oriented along both a and b may describe the CDW order in YBCO.

Finally, in addition to structural distortions, which may provide pinning centres commensurate with the lattice, disorder can also provide random pinning centres for density wave order and has been shown to enhance static SDW and CDW order in 214 cuprates [34–36]. Moreover, 214 cuprates are intrinsically disordered owing to the chemical cation substitution (ex. Sr for La) near the CuO_2 planes used to dope away from half filling. This makes it difficult to disentangle the role of disorder from the intrinsic physics of 214 cuprates. In contrast, the presence of static CDW order in high-purity, oxygen ordered YBCO provides a strong indication that density wave order is in fact an intrinsic feature of underdoped cuprates.

We thank T. Senthil, A. Burkov, S. Wilkins and K. Shen for discussions. This work was supported by the Canada Foundation for Innovation, the Canadian Institute for Advanced Research and the Natural Sciences and Engineering Research Council of Canada. The research described in this paper was performed at the Canadian Light Source, which is supported by NSERC, NRC, CIHR, and the University of Saskatchewan.

-
- [1] T. Wu, H. Mayaffre, S. Krämer, M. Horvatić, C. Berthier, W. N. Hardy, R. Liang, D. A. Bonn, and M.-H. Julien, *Nature*, **477**, 191 (2011).
 - [2] G. Ghiringhelli, M. Le Tacon, M. Minola, S. Blanco-Canosa, C. Mazzoli, N. B. Brookes, G. M. De Luca, A. Frano, D. G. Hawthorn, F. He, T. Loew, M. M. Sala,

- D. C. Peets, M. Salluzzo, E. Schierle, R. Sutarto, G. A. Sawatzky, E. Weschke, B. Keimer, and L. Braicovich, *Science* (2012), doi:10.1126/science.1223532.
- [3] J. Chang, E. Blackburn, A. T. Holmes, N. B. Christensen, J. Larsen, J. Mesot, R. Liang, D. A. Bonn, W. N. Hardy, A. Watenphul, M. Von Zimmermann, E. M. Forgan, and S. M. Hayden, *ArXiv:1206.4333*.
- [4] S. A. Kivelson, I. P. Bindloss, E. Fradkin, V. Oganessian, J. M. Tranquada, A. Kapitulnik, and C. Howald, *Rev. Mod. Phys.*, **75**, 1201 (2003).
- [5] M. Vojta, *Adv. Phys.*, **58**, 699 (2009).
- [6] J. M. Tranquada, B. J. Sternlieb, J. D. Axe, Y. Nakamura, and S. Uchida, *Nature*, **375**, 561 (1995).
- [7] T. Hanaguri, C. Lupien, Y. Kohsaka, D.-H. Lee, M. Azuma, M. Takano, H. Takagi, and J. Davis, *Nature*, **430**, 1001 (2004).
- [8] Y. Kohsaka, C. Taylor, P. Wahl, A. Schmidt, J. Lee, K. Fujita, J. W. Alldredge, K. McElroy, J. Lee, H. Eisaki, S. Uchida, D.-H. Lee, and J. C. Davis, *Nature*, **454**, 1072 (2008).
- [9] D. LeBoeuf, N. Doiron-Leyraud, J. Levallois, R. Daou, J.-B. Bonnemaison, N. E. Hussey, L. Balicas, B. J. Ramshaw, R. Liang, D. A. Bonn, W. N. Hardy, S. Adachi, C. Proust, and L. Taillefer, *Nature*, **450**, 533 (2007).
- [10] N. Doiron-Leyraud, C. Proust, D. LeBoeuf, J. Levallois, J.-B. Bonnemaison, R. Liang, D. A. Bonn, W. N. Hardy, and L. Taillefer, *Nature*, **447**, 563 (2007).
- [11] A. J. Millis and M. R. Norman, *Phys. Rev. B*, **76**, 220503 (2007).
- [12] S. E. Sebastian, G. G. Lonzarich, and N. Harrison, *ArXiv:1112.1373*.
- [13] P. Abbamonte, A. Rusydi, S. Smadici, G. D. Gu, G. A. Sawatzky, and D. L. Feng, *Nat. Phys.*, **1**, 155 (2005).
- [14] J. Fink, E. Schierle, E. Weschke, J. Geck, D. Hawthorn, V. Soltwisch, H. Wadati, H.-H. Wu, H. A. Durr, N. Wizen, B. Buchner, and G. A. Sawatzky, *Phys. Rev. B*, **79**, 100502 (2009).
- [15] J. Fink, V. Soltwisch, J. Geck, E. Schierle, E. Weschke, and B. Büchner, *Phys. Rev. B*, **83**, 092503 (2011).
- [16] S. B. Wilkins, M. P. M. Dean, J. Fink, M. Hücker, J. Geck, V. Soltwisch, E. Schierle, E. Weschke, G. Gu, S. Uchida, N. Ichikawa, J. M. Tranquada, and J. P. Hill, *Phys. Rev. B*, **84**, 195101 (2011).
- [17] A. J. Achkar, F. He, R. Sutarto, J. Geck, H. Zhang, Y.-J. Kim, and D. G. Hawthorn, (2012), *arXiv:1203.2669*.
- [18] N. Nücker, E. Pellegrin, P. Schweiss, J. Fink, S. L. Molodtsov, C. T. Simmons, G. Kaindl, W. Frentrop, A. Erb, and G. Müller-Vogt, *Phys. Rev. B*, **51**, 8529 (1995).
- [19] D. G. Hawthorn, K. M. Shen, J. Geck, D. C. Peets, H. Wadati, J. Okamoto, S.-W. Huang, D. J. Huang, H.-J. Lin, J. D. Denlinger, R. Liang, D. A. Bonn, W. N. Hardy, and G. A. Sawatzky, *Phys. Rev. B*, **84**, 075125 (2011).
- [20] R. Beyers, B. T. Ahn, G. Gorman, V. Y. Lee, S. S. P. Parkin, M. L. Ramirez, K. P. Roche, J. E. Vazquez, T. M. Gür, and R. A. Huggins, *Nature*, **340**, 619 (1989).
- [21] M. v. Zimmermann, J. R. Schneider, T. Frello, N. H. Andersen, J. Madsen, M. K. Il, H. F. Poulsen, R. Liang, P. Dosanjh, and W. N. Hardy, *Phys. Rev. B*, **68**, 104515 (2003).
- [22] H. L. Edwards, A. L. Barr, J. T. Markert, and A. L. de Lozanne, *Phys. Rev. Lett.*, **73**, 1154 (1994).
- [23] B. Grévin, Y. Berthier, and G. Collin, *Phys. Rev. Lett.*, **85**, 1310 (2000).
- [24] D. J. Derro, E. W. Hudson, K. M. Lang, S. H. Pan, J. C. Davis, J. T. Markert, and A. L. de Lozanne, *Phys. Rev. Lett.*, **88**, 097002 (2002).
- [25] M. Fujita, H. Goka, K. Yamada, and M. Matsuda, *Phys. Rev. Lett.*, **88**, 167008 (2002).
- [26] R. Liang, D. A. Bonn, and W. N. Hardy, *Physica C*, **304**, 105 (1998).
- [27] R. Liang, D. A. Bonn, and W. N. Hardy, *Phys. Rev. B*, **73**, 180505 (2006).
- [28] The peaks in Ref. 2 are observed at $H=0.31$ and $K=0.31$ and not at $H=0.30$ and $K=0.30$ as in our measurements. At present, we cannot determine whether this difference is due to the different doping levels of the samples (a truly intrinsic effect) or some minor differences in the alignment of the crystals in the two studies.
- [29] D. G. Hawthorn, F. He, L. Venema, H. Davis, A. J. Achkar, J. Zhang, R. Sutarto, H. Wadati, A. Radi, T. Wilson, G. Wright, K. M. Shen, J. Geck, H. Zhang, V. Novák, and G. A. Sawatzky, *Rev. Sci. Instrum.*, **82**, 073104 (2011).
- [30] We assume only $\sigma\sigma'$ or $\pi\pi'$ scattering is allowed (no magnetic or ATS scattering.).
- [31] As discussed in Ref. 17, the lineshape is insensitive to the magnitude of ΔE provided $\Delta E < 0.2$ eV. As such, ΔE should not be considered a fitting parameter.
- [32] M. Fujita, K. Yamada, H. Hiraka, P. M. Gehring, S. H. Lee, S. Wakimoto, and G. Shirane, *Phys. Rev. B*, **65**, 064505 (2002).
- [33] K. Yamada, C. H. Lee, K. Kurahashi, J. Wada, S. Wakimoto, S. Ueki, H. Kimura, Y. Endoh, S. Hosoya, G. Shirane, R. J. Birgeneau, M. Greven, M. A. Kastner, and Y. J. Kim, *Phys. Rev. B*, **57**, 6165 (1998).
- [34] K. Hirota, *Physica C*, **357 - 360**, 61 (2001).
- [35] M. Fujita, M. Enoki, and K. Yamada, *J. Phys. Chem. Sol.*, **69**, 3167 (2008).
- [36] A. Suchaneck, V. Hinkov, D. Haug, L. Schulz, C. Bernhard, A. Ivanov, K. Hradil, C. T. Lin, P. Bourges, B. Keimer, and Y. Sidis, *Phys. Rev. Lett.*, **105**, 037207 (2010).